Full Spectrum Flow Cytometry for High-Dimensional Immunophenotyping of Mouse Innate Lymphoid Cells

Authors: Kyle T. Mincham[1†], Robert J. Snelgrove[1]

Affiliations:

[1]National Heart and Lung Institute, Imperial College London, London, SW7 2AZ

[†]Corresponding author. Email: k.mincham@imperial.ac.uk Address: National Heart and Lung Institute, Sir Alexander Fleming Building, Imperial College London, South Kensington, London, SW7 2AZ.

Ethical compliance statement: All mouse experiments were performed in accordance with the recommendations in the Guide for the Use of Laboratory Animals of Imperial College London, with the ARRIVE (Animal Research: Reporting of In Vivo Experiments) guidelines. All animal procedures and care conformed strictly to the UK Home Office Guidelines under the Animals (Scientific Procedures) Act 1986, and the protocols were approved by the Home Office of Great Britain.

Purpose and appropriate sample types

This 25-parameter, 22-colour full spectrum flow cytometry panel was designed and optimised for the comprehensive enumeration and functional characterisation of innate lymphoid cell (ILC) subsets in mouse tissues (Table 1). The panel presented here allows the discrimination of ILC progenitors (ILCP), ILC1, ILC2, NCR$^+$ ILC3, NCR$^-$ ILC3, CCR6$^+$ lymphoid tissue-inducer (LTi)-like ILC3 and mature natural killer (NK) cell populations. Further characterisation of ILC and NK cell functional profiles in response to stimulation is provided by the inclusion of subset-specific cytokine markers, and proliferation markers. Development and optimisation of this panel was performed on freshly isolated cells from adult BALB/c lungs and small intestine lamina propria, and *ex vivo* stimulation with phorbol 12-myrisate 13-acetate, ionomycin and pro-ILC activating cytokines.

Background

Innate lymphoid cells (ILCs) are a unique subset of innate effector cells enriched at mucosal surfaces, with diverse roles in host defence, tissue remodelling and repair, inflammation and metabolic homeostasis[1]. Despite lacking rearranged antigen receptors, ILCs display remarkable homology with conventional T helper (Th) type 1 (Th1), Th2 and Th17 cells in regards to phenotype and function, and thus are similarly classified into ILC1, ILC2 and ILC3 subsets[2]. Moreover, *bona fide* ILC subsets have now been expanded to include both cytotoxic natural killer (NK) and lymphoid tissue-inducer (LTi) cells, which are phenotypically and functionally similar to ILC1 and ILC3 respectively, yet exhibit distinct developmental trajectories[3]. However, it is increasingly recognised that ILC subsets are not fixed, and that these cells can exhibit significant plasticity depending on the local inflammatory milieu[4-8]. As such, ILCs demonstrate intra-subset phenotypic heterogeneity depending on their specific microenvironment[9, 10], and deep immunophenotyping therefore requires a comprehensive array of phenotypic and functional markers to accurately capture this biological variation.

Although crucial in multiple biological settings, ILCs constitute a relatively minor population within both mouse and human lymphoid and non-lymphoid tissues and blood, comprising 1-5% of CD45$^+$ leukocytes[5, 11-15]. Due to this inherent scarcity, acquiring as much information as possible on a single-cell level is of upmost importance for accurate ILC discrimination. High resolution ILC characterisation is further convoluted in tissues such as the lung and small

intestine, where the intrinsically autofluorescent nature of the samples results in a heightened background noise-to-signal ratio. With this in mind, cellular characterisation via full spectrum flow cytometry provides a technological advancement given its high parameter capabilities[16] combined with the capacity to extract cellular autofluorescence profiles, thus improving discrimination of rare populations compared to conventional flow cytometry[17]. As such, the full spectrum panel described herein enables the detailed enumeration and functional assessment of all ILC subsets identified within mouse tissues, with a specific focus on the characterisation of lung and small intestine lamina propria (siLP) populations given the divergent repertoire of resident ILC subsets localised to these tissue compartments.

ILCs arise from common lymphoid progenitors within the bone marrow (BM), which through a series of intermediate commitment stages give rise to ILC progenitors (ILCP). While initially believed to be restricted within the BM, ILCPs are now recognised to exist within circulation and as tissue-resident populations at distal sites in both neonates and adults, including the lungs, skin, and secondary lymphoid tissues[18-21]. During early development, expression of the transcription factor promyelocytic leukaemia zinc finger (PLZF; encoded by *Zbtb16*) dictates the bifurcation of innate lymphoid progenitors, whereby PLZF$^+$ ILCPs are restricted to the generation of ILC1, ILC2 and ILC3, but not LTi or NK cells[22, 23]. In addition to PLZF, ILCPs display high-level expression of *Il18r1*, and thus a requirement for IL-18 signalling through IL-18Rα for proliferation and differentiation[19]. Importantly, both ILCPs and mature ILC subset are dependent on canonical IL-7 signalling for development and function, with expression of the receptor (IL-7Rα) and consumption of IL-7 dramatically greater in ILCs than their T cell counterparts[24]. Continual differentiation of IL-7Rα^+PLZF$^+$IL-18Rα^+ ILCP into distinct ILC subsets is under the control of a series of lineage-defining master transcription factors, with all terminal subsets lacking expression of extracellular markers routinely used to identify both lymphoid and myeloid cells, subsequently defining ILCs as lineage negative (Lin$^-$) cells (refer to Table 2 for all appropriate lineage markers).

ILC1s are characterised by their constitutive expression of T-bet (encoded by *Tbx21*), which is central for their production of interferon (IFN)-γ and ensuing response to intracellular pathogens following IL-12 and IL-18 stimulation[18, 25]. Owing to their similarities with cytotoxic

NK cells, ILC1s express NKp46, however tissue-specific distinctions can be made between these two subsets via the preferential expression of CD49a and/or TRAIL by ILC1, in conjunction with the absence of CD11b and CD49b[3, 18, 25].

ILC2s represent the most abundant subset of ILCs in mouse lungs[5] and are dependent on the expression of GATA-3 for maintenance and survival[26, 27]. Analogous to their Th2 counterparts, ILC2s play a key role in controlling helminth infection[26, 28, 29], whilst perpetuating allergen-induced allergic inflammation[30-33] via the production of IL-5 and IL-13 in response to alarmins IL-33, IL-25 and thymic stromal lymphopoietin (TSLP). Given their extensive roles in both immunity and inflammation, ILC2s are known to display dynamic expression of extracellular markers associated with pro-inflammatory functions, exemplified via variations in IL-33 receptor (ST2) and KLRG1 expression depending on the inflammatory signal initiating the primary response[13, 34, 35]. Moreover, the inflammation-dependent plasticity of ILC2s has been demonstrated in both mouse lungs and human peripheral blood, whereby stimulation with IL-1β, IL-12 and IL-18 promotes ILC2s to adopt an ILC1-like transcriptional and functional profile associated with the expression of T-bet (*Tbx21*) and production of IFN-γ[5, 6, 34, 36]. Similarly, human ILC2s, in response to IL-1β and IL-23 stimulation, transdifferentiate into a subset exhibiting ILC3-like characteristics, evidenced by upregulation of the ILC3 signature transcription factor RORγt and production of IL-17[8, 37].

ILC3s are a heterogeneous subset and contribute broad roles in combating against extracellular microbes, including fungi and bacteria, via the production of IL-17A and IL-22 following IL-1β and IL-23-mediated activation[38-40]. Representing the dominant ILC subset within the steady state siLP[41], ILC3s are strictly reliant upon RORγt (encoded by *Rorc*) expression for development and function[39, 42, 43]. However, mouse ILC3s can be further classified into 3 subtypes based on the differential expression of NKp46 and CCR6; namely NKp46^{+}CCR6^{-} (NCR^{+}), NKp46^{-}CCR6^{-} (NCR^{-}) and NKp46^{-}CCR6^{+} (CCR6^{+} LTi-like) ILC3s[42, 44, 45]. Moreover, NCR^{+} ILC3s share transcriptional expression of T-bet with ILC1s, crucial for their expression of NKp46 and endowing them with the ability to produce IFN-γ[46, 47]. Furthermore, stimulation of mouse tissue-specific NCR^{+} ILC3s with IL-12 promotes downregulation of RORγt

and concomitant upregulation of T-bet, further promoting a phenotype associated with IFN-γ^+ ILC1s[4] and demonstrating their plasticity in response to environmental cues.

Given this microenvironmental-driven impact on ILC heterogeneity, the developmental phase of this full spectrum flow cytometry panel involved the prioritisation of definitive ILCP, ILC1, ILC2 and ILC3 transcription factors, as reflected in the gating strategy (Figure 1). An added benefit of full spectrum flow cytometry is the ability to remove red blood cell contamination by plotting side-scatter (SSC) captured by the 405nm violet laser against SSC-B from the 488nm blue laser[48] (Figure 1A), thus ensuring purity of downstream terminal cell populations. Viable leukocytes (LIVE/DEAD Blue$^-$ CD45$^+$; Figure 1A) were selected and total ILCs were defined by their expression of IL-7Rα^+ and lack of lineage markers used to routinely define T cells, B cells, myeloid cells, and red blood cells (CD3, CD4, CD5, CD11b, CD11c, CD19, B220, F4/80, FcεR1, Gr1, TCRβ, TCR$\gamma\delta$, Ter119; Figure 1B). ILCPs within the lung were characterised by their ubiquitous expression of PLZF, in combination with IL-18Rα^+ (Figure 1C). Mature ILC subsets within the lung (Figure 1D) and siLP (Figure 1E) were stratified as T-bet$^+$RORγt$^-$ST2$^-$ CD49b$^-$IL-18Rα^+NKp46$^+$CD49a$^{+/-}$TRAIL$^{+/-}$ ILC1s, GATA-3$^+$T-bet$^-$RORγt$^-$KLRG1$^{+/-}$ST2$^{+/-}$ ILC2s and either RORγt$^+$T-bet$^{+/-}$NKp46$^+$CCR6$^-$ (NCR$^+$), RORγt$^+$T-bet$^{+/-}$NKp46$^-$CCR6$^-$ (NCR$^-$) or RORγt$^+$T-bet$^{+/-}$NKp46$^-$CCR6$^+$ (CCR6$^+$ LTi-like) ILC3s. Regarding ILC2s, it is important to note that ST2 expression on *ex vivo* stimulated siLP ILC2s is largely absent (Figure 1E)[9, 49]. Moreover, while lung ILCs lack CD4 expression[50], intestinal CCR6$^+$ LTi-like ILC3s can be sub-classified as CD4$^+$ and CD4$^-$[51]. As such, the inclusion of CD4 within the lineage cocktail may influence the characterisation of ILC3 subsets on a tissue-specific basis. ILC cytokine production and proliferation within the lung (Figure 1F) and siLP (Figure 1G) was assessed in response to subset-specific activation signals via *ex vivo* stimulation with phorbol 12-myrisate 13-acetate (PMA), Ionomycin and Brefeldin A, and either IL-12 and IL-18 (pro-ILC1), IL-33 (pro-ILC2) or IL-1β and IL-23 (pro-ILC3). Stimulation with ILC subset-specific cytokines clearly demonstrates a heightened propensity for IL-13 and IL-22 production by siLP ILC2s and ILC3 subsets respectively, whereas lung ILC1s significantly upregulate IFN-γ compared to their siLP counterparts. Although the focus of this panel was to accurately define ILCPs and ILC1-3 subsets, inclusion of CD11b within the lineage cocktail enables the enumeration of conventional mature CD11b$^+$NKp46$^+$T-bet$^+$ NK cells (Figure 1H)[52], with additional

characterisation of lung tissue-resident (trNK) and circulating (cNK) populations on the basis of CD49a and CD49b expression[53] (Figure 1H). Markers including KLRG1[54] and RORγt[55], and cytokines IFN-γ, IL-5, IL-13[56] and IL-22[57] are all reportedly expressed by NK cell subsets based on maturation, tissue localisation and disease state, further highlighting the diversity of this OMIP.

In summary, we present here the first full spectrum flow cytometry panel (Table 2) to comprehensively profile the phenotypic and functional state of ILCs in multiple mouse tissues. Moreover, by maintaining availability on the 355nm ultraviolet laser, this panel can be expanded to incorporate additional markers of interest with little impact on the overall Complexity™ Index (a value of how distinct a collection of spectral signatures are from one other when unmixed simultaneously), thereby providing a valuable resource within the rapidly expanding field of ILC biology.

Acknowledgement

The authors would like to thank Dr James Harker and the Imperial College London Flow Cytometry Facility South Kensington for their valuable advice on Cytek® Aurora operation during the initial design of this panel. In addition, the authors would like to thank Christopher McRandle and Dr Adam Davison from Cytek® Biosciences for their advice on data quality control using SpectroFlo® software. The authors acknowledge financial support from Imperial College London through an Imperial College Research Fellowship grant awarded to K.T.M. R.J.S. is a Wellcome Trust Senior Research Fellow in Basic Biomedical Sciences (209458/Z/17/Z). Parts of this work were also funded through a Rosetrees Trust/The Stoneygate Trust Project Grant (PGS21/10072).

Conflict of interest: The author declare that no conflicts of interest exist.

Literature Cited

1. Klose CSN, et al. Innate lymphoid cells as regulators of immunity, inflammation and tissue homeostasis. Nat Immunol. 2016;17(7):765.

2. Spits H, et al. Innate lymphoid cells — a proposal for uniform nomenclature. Nature Reviews Immunology. 2013;13(2):145.

3. Vivier E, et al. Innate Lymphoid Cells: 10 Years On. Cell. 2018;174(5):1054.

4. Vonarbourg C, et al. Regulated Expression of Nuclear Receptor RORγt Confers Distinct Functional Fates to NK Cell Receptor-Expressing RORγt+ Innate Lymphocytes. Immunity. 2010;33(5):736.

5. Silver JS, et al. Inflammatory triggers associated with exacerbations of COPD orchestrate plasticity of group 2 innate lymphoid cells in the lungs. Nat Immunol. 2016;17(6):626.

6. Bal SM, et al. IL-1β, IL-4 and IL-12 control the fate of group 2 innate lymphoid cells in human airway inflammation in the lungs. Nat Immunol. 2016;17(6):636.

7. Bernink Jochem H, et al. Interleukin-12 and -23 Control Plasticity of CD127+ Group 1 and Group 3 Innate Lymphoid Cells in the Intestinal Lamina Propria. Immunity. 2015;43(1):146.

8. Bernink JH, et al. c-Kit-positive ILC2s exhibit an ILC3-like signature that may contribute to IL-17-mediated pathologies. Nat Immunol. 2019;20(8):992.

9. Meininger I, et al. Tissue-Specific Features of Innate Lymphoid Cells. Trends Immunol. 2020;41(10):902.

10. Loering S, et al. Differences in pulmonary group 2 innate lymphoid cells are dependent on mouse age, sex and strain. Immunol Cell Biol. 2021;99(5):542.

11. Mackley EC, et al. CCR7-dependent trafficking of RORγ+ ILCs creates a unique microenvironment within mucosal draining lymph nodes. Nature Communications. 2015;6(1):5862.

12. Gronke K, et al. Isolation and Flow Cytometry Analysis of Innate Lymphoid Cells from the Intestinal Lamina Propria. Methods Mol Biol. 2017;1559:255.

13. Entwistle LJ, et al. Pulmonary Group 2 Innate Lymphoid Cell Phenotype Is Context Specific: Determining the Effect of Strain, Location, and Stimuli. Front Immunol. 2020;10:3114.

14. Vély F, et al. Evidence of innate lymphoid cell redundancy in humans. Nat Immunol. 2016;17(11):1291.

15. Bennstein SB, et al. Umbilical cord blood-derived ILC1-like cells constitute a novel precursor for mature KIR+NKG2A- NK cells. eLife. 2020;9:e55232.

16. Park LM, et al. OMIP-069: Forty-Color Full Spectrum Flow Cytometry Panel for Deep Immunophenotyping of Major Cell Subsets in Human Peripheral Blood. Cytometry Part A. 2020;97(10):1044.

17. Niewold P, et al. Evaluating spectral cytometry for immune profiling in viral disease. Cytometry Part A. 2020;97(11):1165.

18. Klose CSN, et al. Differentiation of type 1 ILCs from a common progenitor to all helper-like innate lymphoid cell lineages. Cell. 2014;157(2):340.

19. Ghaedi M, et al. Single-cell analysis of RORα tracer mouse lung reveals ILC progenitors and effector ILC2 subsets. J Exp Med. 2020;217(3).

20. Zeis P, et al. In Situ Maturation and Tissue Adaptation of Type 2 Innate Lymphoid Cell Progenitors. Immunity. 2020;53(4):775.
21. Lim AI, et al. Systemic Human ILC Precursors Provide a Substrate for Tissue ILC Differentiation. Cell. 2017;168(6):1086.
22. Constantinides MG, et al. A committed precursor to innate lymphoid cells. Nature. 2014;508(7496):397.
23. Ishizuka IE, et al. Single-cell analysis defines the divergence between the innate lymphoid cell lineage and lymphoid tissue-inducer cell lineage. Nat Immunol. 2016;17(3):269.
24. Martin CE, et al. Interleukin-7 Availability Is Maintained by a Hematopoietic Cytokine Sink Comprising Innate Lymphoid Cells and T Cells. Immunity. 2017;47(1):171.
25. Weizman OE, et al. ILC1 Confer Early Host Protection at Initial Sites of Viral Infection. Cell. 2017;171(4):795.
26. Hoyler T, et al. The Transcription Factor GATA-3 Controls Cell Fate and Maintenance of Type 2 Innate Lymphoid Cells. Immunity. 2012;37(4):634.
27. Mjösberg J, et al. The Transcription Factor GATA3 Is Essential for the Function of Human Type 2 Innate Lymphoid Cells. Immunity. 2012;37(4):649.
28. Moro K, et al. Innate production of TH2 cytokines by adipose tissue-associated c-Kit+Sca-1+ lymphoid cells. Nature. 2010;463(7280):540.
29. Neill DR, et al. Nuocytes represent a new innate effector leukocyte that mediates type-2 immunity. Nature. 2010;464(7293):1367.
30. Patel DF, et al. Neutrophils restrain allergic airway inflammation by limiting ILC2 function and monocyte–dendritic cell antigen presentation. Sci Immunol. 2019;4(41):eaax7006.
31. Halim TYF, et al. Lung natural helper cells are a critical source of Th2 cell-type cytokines in protease allergen-induced airway inflammation. Immunity. 2012;36(3):451.
32. Bartemes KR, et al. Enhanced innate type 2 immune response in peripheral blood from patients with asthma. J Allergy Clin Immunol. 2014;134(3):671.
33. Puttur F, et al. Pulmonary environmental cues drive group 2 innate lymphoid cell dynamics in mice and humans. Sci Immunol. 2019;4(36):eaav7638.
34. Huang Y, et al. IL-25-responsive, lineage-negative KLRG1(hi) cells are multipotential 'inflammatory' type 2 innate lymphoid cells. Nat Immunol. 2015;16(2):161.
35. Li BWS, et al. Group 2 Innate Lymphoid Cells Exhibit a Dynamic Phenotype in Allergic Airway Inflammation. Front Immunol. 2017;8:1684.
36. Ohne Y, et al. IL-1 is a critical regulator of group 2 innate lymphoid cell function and plasticity. Nat Immunol. 2016;17(6):646.
37. Ohne Y. OMIP-066: Identification of Novel Subpopulations of Human Group 2 Innate Lymphoid Cells in Peripheral Blood. Cytometry Part A. 2020;97(10):1028.
38. Gladiator A, et al. Cutting edge: IL-17-secreting innate lymphoid cells are essential for host defense against fungal infection. J Immunol. 2013;190(2):521.
39. Buonocore S, et al. Innate lymphoid cells drive interleukin-23-dependent innate intestinal pathology. Nature. 2010;464(7293):1371.

40. Van Maele L, et al. Activation of Type 3 Innate Lymphoid Cells and Interleukin 22 Secretion in the Lungs During Streptococcus pneumoniae Infection. The Journal of Infectious Diseases. 2014;210(3):493.
41. Dutton EE, et al. Identification of Murine Innate Lymphoid Cell Subsets in Barrier Tissues and Their Draining Lymph Nodes Using Flow Cytometry. Methods Mol Biol. 2020;2121:23.
42. Sanos SL, et al. RORgammat and commensal microflora are required for the differentiation of mucosal interleukin 22-producing NKp46+ cells. Nat Immunol. 2009;10(1):83.
43. Satoh-Takayama N, et al. Microbial Flora Drives Interleukin 22 Production in Intestinal NKp46+ Cells that Provide Innate Mucosal Immune Defense. Immunity. 2008;29(6):958.
44. Luci C, et al. Influence of the transcription factor RORgammat on the development of NKp46+ cell populations in gut and skin. Nat Immunol. 2009;10(1):75.
45. Valle-Noguera A, et al. Optimized Protocol for Characterization of Mouse Gut Innate Lymphoid Cells. Front Immunol. 2020;11:563414.
46. Klose CSN, et al. A T-bet gradient controls the fate and function of CCR6−RORγt+ innate lymphoid cells. Nature. 2013;494(7436):261.
47. Rankin LC, et al. The transcription factor T-bet is essential for the development of NKp46+ innate lymphocytes via the Notch pathway. Nat Immunol. 2013;14(4):389.
48. Sahir F, et al. Development of a 43 color panel for the characterization of conventional and unconventional T-cell subsets, B cells, NK cells, monocytes, dendritic cells, and innate lymphoid cells using spectral flow cytometry. Cytometry A. 2020.
49. Ricardo-Gonzalez RR, et al. Tissue signals imprint ILC2 identity with anticipatory function. Nat Immunol. 2018;19(10):1093.
50. Monticelli LA, et al. Innate lymphoid cells promote lung-tissue homeostasis after infection with influenza virus. Nat Immunol. 2011;12(11):1045.
51. Melo-Gonzalez F, et al. Functional and phenotypic heterogeneity of group 3 innate lymphoid cells. Immunology. 2017;150(3):265.
52. Kim S, et al. In vivo developmental stages in murine natural killer cell maturation. Nat Immunol. 2002;3(6):523.
53. Sojka DK, et al. Tissue-resident natural killer (NK) cells are cell lineages distinct from thymic and conventional splenic NK cells. Elife. 2014;3:e01659.
54. Huntington ND, et al. NK Cell Maturation and Peripheral Homeostasis Is Associated with KLRG1 Up-Regulation. J Immunol. 2007;178(8):4764.
55. Sanos SL, et al. Isolation of NK cells and NK-like cells from the intestinal lamina propria. Methods Mol Biol. 2010;612:505.
56. Culley FJ. Natural killer cells in infection and inflammation of the lung. Immunology. 2009;128(2):151.
57. Kumar P, et al. IL-22 from conventional NK cells is epithelial regenerative and inflammation protective during influenza infection. Mucosal Immunol. 2013;6(1):69.

Figure 1. Gating strategy to characterise ILC populations and their subset-specific cytokine and proliferative profiles. After exclusion of cellular debris, doublets, red blood cell contamination and non-viable $CD45^{+/-}$ cells, viable $CD45^{+}$ leukocytes **(A)** were gated on IL-7Rα and lineage (CD3, CD4, CD5, CD11b, CD11c, CD19, B220, F4/80, FcεR1, Gr1, TCRβ, TCRγδ, Ter119; Lin) negative cells to identify ILCs **(B)**. ILCPs were then identified as IL-$18R\alpha^{+}PLZF^{+}$ cells **(C)**. Characterisation of ILC1, ILC2, NCR^{+}, NCR^{-} and $CCR6^{+}$ LTi-like ILC3 subsets in the lung **(D)** and siLP **(E)**. All samples in panel A-E were *ex vivo* stimulated for 5 hours with PMA/Ionomycin/BFA. Single cell suspensions were *ex vivo* stimulated for 5 hours with PMA/Ionomycin/BFA and either IL-12 and IL-18 (pro-ILC1), IL-33 (pro-ILC2) or IL-1β and IL-23 (pro-ILC3) and ILC subsets were assessed for production of subset-specific cytokines (IFN-γ, IL-5, IL-13, IL-17A and IL-22) and cellular proliferation (Ki-67) within the lung **(F)** and siLP **(G)**. **(H)** Identification of NK cells within the lung and siLP, with downstream characterisation of lung tissue-resident NK (trNK) and circulating NK (cNK) cells. Plots in panel A-C are representative of individual lung samples. For panels B-H, viable leukocytes from 3 technical lung or siLP replicates were concatenated into single FCS files prior to gating. All fluorochrome-conjugated antibodies were titrated (Online Figure 1) during panel optimisation and manual gating was determined using fluorescence minus one controls (Online Figure 2) where necessary.

Table 1. Summary Table

Purpose	Deep immunophenotyping and functional assessment of ILC subsets
Species	Mouse
Cell types	Innate Lymphoid Cells
Cross-reference	N/A

Table 2. Reagents used for OMIP

Specificity	Fluorochrome	Clone	Purpose
CD45	BUV395	30-F11	Pan leukocytes
IL-7Rα	PE-Cy5	SB/199	Pan ILC
PLZF	PE	MAGS21F7	ILCP
IL-18Rα	PerCP-eFluor 710	P3TUNYA	ILCP and ILC1
T-bet	BV421	4B10	ILC1 and ILC3 subsets
NKp46	PE/Dazzle 594	29A1.4	ILC1, ILC3 subsets and NK cells
CD49a	BUV496	Ha31/8	ILC1 subsets and trNK cells
TRAIL	PE-Cy7	N2B2	ILC1 subsets
IFN-γ	BUV737	XMG1.2	ILC1 and NK cells
GATA-3	BB700	L50-823	ILC2
KLRG1	BV480	2F1	ILC2
ST2	R718	U29-93	ILC2
IL-5	APC	TRFK5	ILC2
IL-13	eFluor 450	eBio13A	ILC2
RORγt	BV786	Q31-378	ILC3
CCR6	BV711	140706	ILC3 subsets
IL-17A	BV650	TC11-18H10.1	ILC3
IL-22	Alexa Fluor 647	Poly5164	ILC3
CD49b	eFluor 506	DX5	NK cells
Ki-67	Alexa Fluor 532	SolA15	Proliferating cells
B220	FITC	RA3-6B2	B cell subsets (Lin dump)
CD3	FITC	145-2C11	T cell subsets (Lin dump)
CD4	FITC	GK1.5	T cell subsets (Lin dump)
CD5	FITC	53-7.3	T cell and B cell subsets (Lin dump)
CD11b	FITC	M1/70	Myeloid/NK/Granulocytes (Lin dump)
CD11c	FITC	N418	Myeloid cells/Granulocytes (Lin dump)
CD19	FITC	1D3/CD19	B cell subsets (Lin dump)
F4/80	FITC	BM8	Macrophages (Lin dump)
FcεR1α	FITC	MAR-1	Mast cells and Basophils (Lin dump)
Gr-1	FITC	RB6-85C	Myeloid cells/Granulocytes (Lin dump)
TCRβ	FITC	H57-597	αβ T-cells (Lin dump)
TCRγδ	FITC	UC7-13D5	γδ T-cells (Lin dump)
Ter119	FITC	TER-119	Red blood cells (Lin dump)
Dead cells	LIVE/DEAD™ Blue	-	Viable cells

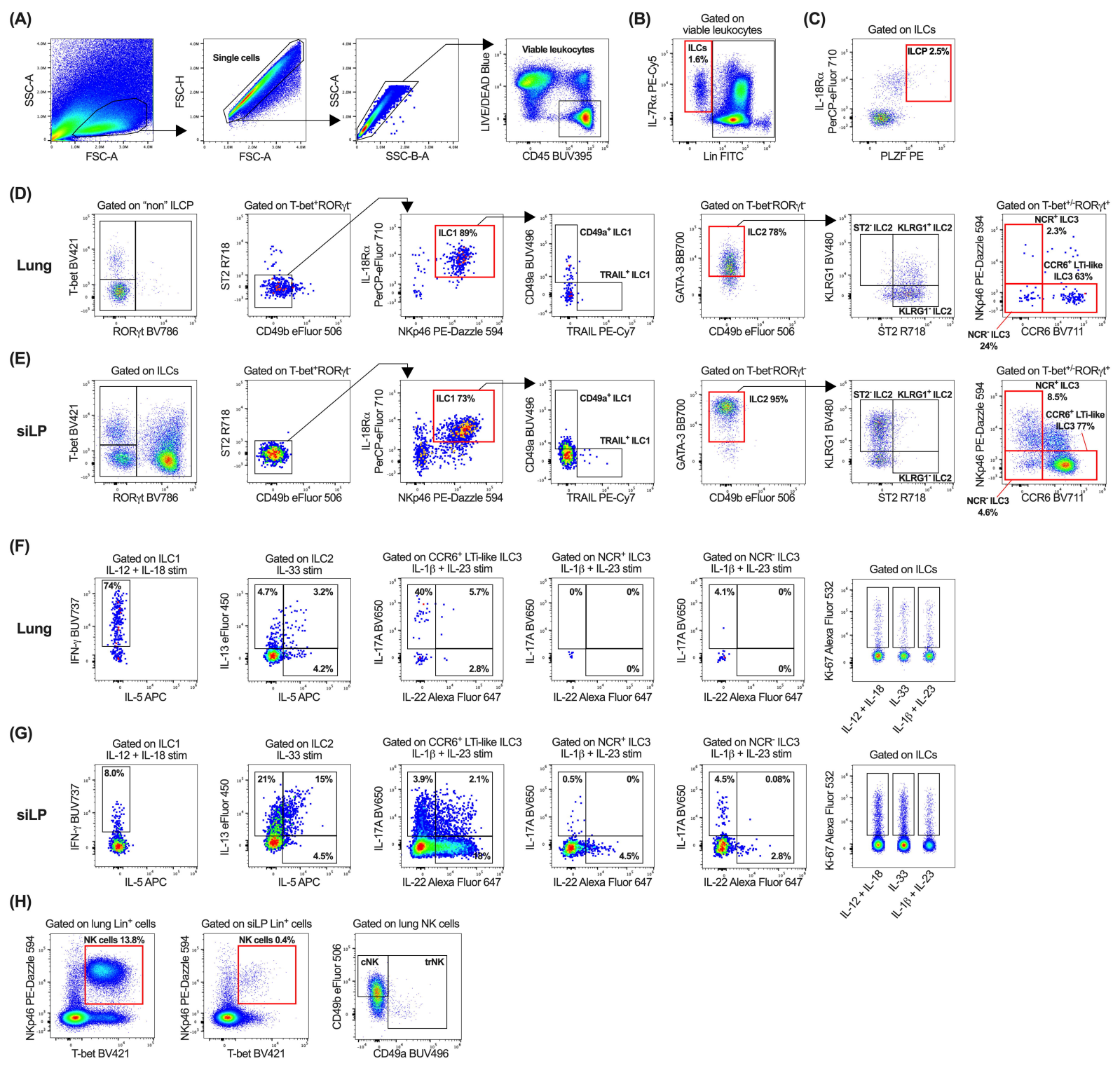
(A)
SSC-A
FSC-A
Single cells
FSC-H
FSC-A
SSC-A
SSC-B-A
Viable leukocytes
LIVE/DEAD Blue
CD45 BUV395
(B)
Gated on viable leukocytes
ILCs 1.6%
IL-7Rα PE-Cy5
Lin FITC
(C)
Gated on ILCs
ILCP 2.5%
IL-18Rα PerCP-eFluor 710
PLZF PE
(D)
Lung
Gated on "non" ILCP
T-bet BV421
RORγt BV786
Gated on T-bet+RORγt-
ST2 R718
CD49b eFluor 506
ILC1 89%
IL-18Rα PerCP-eFluor 710
NKp46 PE-Dazzle 594
CD49a+ ILC1
TRAIL+ ILC1
CD49a BUV496
TRAIL PE-Cy7
Gated on T-bet-RORγt-
ILC2 78%
GATA-3 BB700
CD49b eFluor 506
ST2- ILC2
KLRG1+ ILC2
KLRG1- ILC2
KLRG1 BV480
ST2 R718
Gated on T-bet+/-RORγt+
NCR+ ILC3 2.3%
CCR6+ LTi-like ILC3 63%
NCR- ILC3 24%
NKp46 PE-Dazzle 594
CCR6 BV711
(E)
siLP
Gated on ILCs
T-bet BV421
RORγt BV786
Gated on T-bet+RORγt-
ST2 R718
CD49b eFluor 506
ILC1 73%
IL-18Rα PerCP-eFluor 710
NKp46 PE-Dazzle 594
CD49a+ ILC1
TRAIL+ ILC1
CD49a BUV496
TRAIL PE-Cy7
Gated on T-bet-RORγt-
ILC2 95%
GATA-3 BB700
CD49b eFluor 506
ST2- ILC2
KLRG1+ ILC2
KLRG1- ILC2
KLRG1 BV480
ST2 R718
Gated on T-bet+/-RORγt+
NCR+ ILC3 8.5%
CCR6+ LTi-like ILC3 77%
NCR- ILC3 4.6%
NKp46 PE-Dazzle 594
CCR6 BV711
(F)
Lung
Gated on ILC1 IL-12 + IL-18 stim
74%
IFN-γ BUV737
IL-5 APC
Gated on ILC2 IL-33 stim
4.7%
3.2%
4.2%
IL-13 eFluor 450
IL-5 APC
Gated on CCR6+ LTi-like ILC3 IL-1β + IL-23 stim
40%
5.7%
2.8%
IL-17A BV650
IL-22 Alexa Fluor 647
Gated on NCR+ ILC3 IL-1β + IL-23 stim
0%
0%
0%
IL-17A BV650
IL-22 Alexa Fluor 647
Gated on NCR- ILC3 IL-1β + IL-23 stim
4.1%
0%
0%
IL-17A BV650
IL-22 Alexa Fluor 647
Gated on ILCs
Ki-67 Alexa Fluor 532
IL-12 + IL-18
IL-33
IL-1β + IL-23
(G)
siLP
Gated on ILC1 IL-12 + IL-18 stim
8.0%
IFN-γ BUV737
IL-5 APC
Gated on ILC2 IL-33 stim
21%
15%
4.5%
IL-13 eFluor 450
IL-5 APC
Gated on CCR6+ LTi-like ILC3 IL-1β + IL-23 stim
3.9%
2.1%
18%
IL-17A BV650
IL-22 Alexa Fluor 647
Gated on NCR+ ILC3 IL-1β + IL-23 stim
0.5%
0%
4.5%
IL-17A BV650
IL-22 Alexa Fluor 647
Gated on NCR- ILC3 IL-1β + IL-23 stim
4.5%
0.08%
2.8%
IL-17A BV650
IL-22 Alexa Fluor 647
Gated on ILCs
Ki-67 Alexa Fluor 532
IL-12 + IL-18
IL-33
IL-1β + IL-23
(H)
Gated on lung Lin+ cells
NK cells 13.8%
NKp46 PE-Dazzle 594
T-bet BV421
Gated on siLP Lin+ cells
NK cells 0.4%
NKp46 PE-Dazzle 594
T-bet BV421
Gated on lung NK cells
cNK
trNK
CD49b eFluor 506
CD49a BUV496